JOURNAL OF AGRICULTURAL AND FOOD CHEMISTRY

pubs.acs.org/JAFC Article

Functional Characterization of Two Carboxylesterase Genes Involved in Pyrethroid Detoxification in *Helicoverpa armigera*

Yong-Qiang Li, Li-Sha Bai, Cai-Xia Zhao, Jing-Jing Xu, Zhong-Juan Sun, Yan-Ling Dong, De-Xian Li, Xi-Li Liu, and Zhi-Qing Ma*

Cite This: *J. Agric. Food Chem.* 2020, 68, 3390−3402 Read Online

ABSTRACT: Insect carboxylesterases are major enzymes involved in metabolism of xenobiotics including insecticides. Two carboxylesterase genes, *CarE001A* and *CarE001H*, were cloned from the destructive agricultural pest *Helicoverpa armigera*. Quantitative real-time polymerase chain reaction showed that *CarE001A* and *CarE001H* were predominantly expressed in fat body and midgut, respectively; developmental expression analyses found that the expression levels of both CarEs were significantly higher in fifth-instar larvae than in other life stages. Recombinant CarE001A and CarE001H expressed in the *Escherichia coli* exhibited high enzymatic activity toward α-naphthyl acetate. Inhibition assays showed that organophosphates had strong inhibition on CarEs activity compared to pyrethroids. Metabolism assays indicated that CarE001A and CarE001H were able to metabolize β-cypermethrin and λ-cyhalothrin. Homology modeling and molecular docking analyses demonstrated that β-cypermethrin could fit nicely into the active pocket of both carboxylesterases. These results suggested that *CarE001A* and *CarE001H* could play important roles in the detoxification of pyrehtroids in *H. armigera*.

KEYWORDS: *carboxylesterases, Helicoverpa armigera, expression profiles, pyrethroid detoxification, inhibition properties*

INTRODUCTION

The cotton bollworm, *Helicoverpa armigera* (Hübner), is one of the most devastating insect pest, feeding on hundreds of crops and wild plant species around the world.[1] Due to its characteristics of being polyphagous, high mobility, high fecundity, and facultative diapaus, this pest has a major pest status and has caused severe economic losses in many crops, especially cotton (*Gossypium* spp).[2] Pyrethroids, organophosphates, and carbamates are usually the main classes of chemical insecticides used for bollworm control.[3] Although the extensive adoption of transgenic Bt cotton for bollworm control has reduced the use of chemical insecticides over the last 20 years, various studies have demonstrated that it has evolved resistance to some commercial chemical insecticides across the globe, such as in Australia, Asia, Europe, and Africa.[2−5] Three major classes of detoxification enzymes, including cytochrome P450s (CYPs), carboxylesterases (CarEs), and glutathione S-transferases (GSTs), are principally responsible for the detoxification of xenobiotic chemical compounds, and their evolution can lead to increased insecticide resistance among insects, such as *H. armigera*.[6−9]

CarEs (EC3.1.1.1) belong to a large superfamily of α/β hydrolase proteins and can catalyze the hydrolysis of carboxyl esters into alcohols and carboxylic acids.[10,11] They are a major class of metabolic enzymes and play key roles in the detoxification of many agrochemicals, such as pyrethroids, organophosphates, and carbamates in a wide variety of pest species.[11,12] For example, LmCesA4 and LmCesA5 from *Locusta migratoria* have been demonstrated to be involved in the detoxification of deltamethrin, chlorpyrifos, and carbaryl.[13] CpCE-1 from *Cydia pomonella*,[14] E3 from *Lucillia cuprina*,[15] and Cqestβ2 from *Culex quinquefasciatus*[16] were shown to have metabolic activities toward acephate, chlorfenvinphos, and so on. Additionally, some studies showed that CarEs were implicated in metabolic resistance to pyrethroids and organophosphates in various insects species, such as *H. armigera*,[17,18] *Aphis gossypii*,[6] *Nilaparvata lugens*,[19] *Bactrocera dorsalis*,[20] *Musca domestica*,[21] and *Plutella xylosterlla*.[22] It is well known that CarE-mediated metabolic resistance to pesticides can generally occur through (1) improvement of the sequestration of insecticides with gene overexpression and (2) enhancement of the metabolism of insecticides with mutation.[23] For example, in *L. cuprina*, a single amino acid substitution (Gly to Asp) at the 137th position of an α-esterase gene (*LcaE7*) confers resistance to organophosphates.[15,24] However, in *A. gossypii*, the resistance to deltamethrin is caused by the overexpression of several CarE genes.[25]

In *H. armigera*, CarE-mediated insecticide resistance has been documented in a lot of reports in the past several decades.[3,26] For example, some earlier studies on field populations of *H. armigera* in Australia revealed that increased CarE activities were responsible for the resistance to fenvalerate and organophosphorus.[15,27] Recent studies on two laboratory-selected cotton bollworm strains in China further suggested that several overexpressed CarEs were

Received: October 24, 2019
Revised: February 21, 2020
Accepted: February 25, 2020
Published: February 25, 2020

https://dx.doi.org/10.1021/acs.jafc.9b06690
J. Agric. Food Chem. 2020, 68, 3390−3402

involved in fenvalerate and monocrotophos resistance and the preparation of enzyme from the tissue of fenvalerate resistant strain showed metabolic activity toward fenvalerate.[17,18] Additionally, in a high-performance liquid chromatography (HPLC) analysis, it was also shown that crude homogenates isolated from the midgut of *H. armigera* could metabolize several types of pyrethroids into small compounds.[12] However, implications of CarEs in insecticide resistance or metabolism in cotton bollworm were largely derived from observations of synergistic effects of CarE inhibitors [i.e., *S*,*S*,*S*-tributyl phosphorothrithioate (DEF)], enhancement of esterase activities against artificial substrates (i.e., α/β-naphthyl acetate), and over transcription of mRNA in resistant strains. Although there are approximate 40 CarE genes that have been found in the genome of *H. armigera* and a few CarE genes have been demonstrated to be involved in insecticide resistance,[17,18,28] detailed information about the capacity of individual CarEs in insecticide metabolism and their expression patterns, inhibitory profiles, and kinetic properties is still very limited until now.

In this study, two CarE genes (*CarE001A* and *CarE001H*) were cloned from *H. armigera*, and their expression profiles in different tissues and developmental stages were analyzed by quantitative real-time polymerase chain reaction (qRT-PCR). Both CarEs were functionally expressed in the *Escherichia coli* (*E. coli*) system. Kinetic analyses with α-naphthyl acetate (α-NA) and inhibition properties of insecticides were investigated by using a spectrophotometer. The metabolic activities of both CarEs toward three types of pyrethroids including β-cypermethrin, λ-cyhalothrin, and fenvalerate insecticides were measured by using HPLC assays. Homology modeling, molecular docking, and molecular dynamics (MD) simulations with the most commonly used β-cypermethrin were also performed to explore the molecular mechanism of detoxification function of CarEs in *H. armigera*.

■ MATERIALS AND METHODS

Insects Rearing and Chemicals. A laboratory colony of *H. armigera* was established from a field collection from Wuhan, Hubei Province of China.[29] The insects were reared on artificial diet in 24-well plates (first- to third-instar larvae) and 6-well plates (fourth- to fifth-instar larvae) at 28 ± 1 °C, 70 ± 10% relative humidity, and a photoperiod of 16:8 h (L/D). All the chemical insecticides, including β-cypermethrin, λ-cyhalothrin, fenvalerate, chlorpyrifos, parathion-methyl and paraoxon-ethyl, and triphenyl phosphate (TPP), were of analytical standard and purchased from Aladdin Industrial Corporation (Shanghai, China). Model substrate α-NA, its metabolite α-naphthol, and Fast Blue RR salt were also obtained from Aladdin Industrial Corporation. The stained protein ladder was provided by Sangon Company (Shanghai, China).

Total RNA Isolation and cDNA Synthesis. Total RNA was isolated from each sample using the SV Total RNA Isolation System kit (Promega, USA) according to the manufacturer's instructions. The quality and concentration of total RNA were determined by agarose gel electrophoresis and measurements with a NanoDrop spectrophotometer (NanoDrop Technologies, Inc., USA). Two micrograms of RNA was used to synthesize the first-strand cDNA using RevertAid First Strand cDNA Synthesis kit (Thermo Fisher Scientific, USA). The synthesized cDNA was used as a template for PCRs.

Cloning of Both CarE Genes from *H. armigera*. The open reading frames (ORFs) of *CarE001A* and *CarE001H* were amplified with gene-specific primers (Table S1) by using the PrimeSTAR HS DNA polymerase (TaKaRa, Japan). PCR reaction mixtures (25 μL) contained 1 μL of template cDNA, 1.5 μL of each primers (10 μM), 2 μL of dNTP (2.5 mM), 5 μL of 5× PrimeSTAR buffer (Mg^{2+} plus), and 0.25 μL of PrimeSTAR HS DNA polymerase. The amplification program was 98 °C for 30 s, followed by 30 cycles of 98 °C for 12 s, 65 °C for 25 s, 72 °C for 2 min, and with a final extension of 72 °C for 5 min. After the PCR products were purified by using Omega Gel Extraction kit (Omega Bio-tek, Inc., USA), an adenine (A) was added at the 3′ terminus by using the DNA A-Tailing kit (Takara, Japan). The amplifications were ligated into the pGEM-T Easy vector (Promega, USA) and transformed into the *E. coli* JM109 competent cells for blue-white plaque selection. Positive clones were selected to amplify the recombinant plasmids and subsequently sequenced by Invitrogen Company (Shanghai, China).

Genomic DNA Extraction and Sequencing. Genomic DNA extraction was conducted according to the method of Yuan et al.[30] with slight modification. Individual fifth-instar larvae were ground with liquid nitrogen, followed by adding 500 μL of hot DNA lysis buffer (50 mM Tris−HCl, 100 mM EDTA, 100 mM NaCl, 5% SDS, pH 8.0). The homogenates were extracted three times with 350 μL of phenol plus 300 μL of chloroform and then centrifuged at 12,000 rpm for 10 min. The supernatant was collected and DNA was precipitated using 850 μL of ammonium acetate-cold ethanol (1:16, v/v). The DNA pellet was resuspended and washed by 500 μL of 70% ethanol. After centrifugation at 12,000 rpm, the DNA pellet was recovered in 50 μL of nuclease-free water and stored at −70 °C for use.

Genomic DNA of *CarE001A* and *CarE001H* in *H. armigera* WH strain was amplified with primers designed according to their corresponding cDNA sequences. The primers are shown in Table S1. The thermocycler program was 98 °C for 1 min, followed by 30 cycles of 98 °C for 12 s, 65 °C for 25 s, 72 °C for 4 min, and with a final extension of 72 °C for 5 min. PCR products were purified and ligated into a pGEM-T Easy vector and subsequently sequenced by Invitrogen Company according to the above protocols for cloning of CarE genes.

Sequence Analyses. The known CarEs of different insect species were obtained from GenBank and previous reports. Alignment of deduced amino acid sequences was made with GENEDOC software (https://genedoc.software.informer.com/2.7/). A phylogenetic tree was constructed with the MEGA 7.0 software adopting the neighbor-joining algorithm with the bootstrap of 1000 replications.[31] The ExPASy web tool (https://web.expasy.org/compute_pi/) was used to compute the molecular weight and theoretical isoelectric point. Signal peptides and protein glycosylation were predicted with the SignalP-5.0 server (http://www.cbs.dtu.dk/services/SignalP/) and the NetNGlyc1.0 server (http://www.cbs.dtu.dk/services/NetNGlyc/), respectively.

Expression Profiles of *CarE001A* and *CarE001H*. Six selected tissues including head (HE), foregut (FG), midgut (MG), hindgut (HG), malpighian tubules (MT), and fat body (FB) were dissected from the fourth-instar larvae on day 2. Total RNA of each tissue was prepared from about 20 fourth-instar larvae for each replicate. Total RNA was also isolated from 100 eggs (EG), 20 larvae of the first- to third-instar (L1−L3), 5 larvae of the fourth- and fifth-instar (L4−L5), 5 pupas (PU), and 5 adults (AD). The cDNA templates were synthesized as described above. Three independent biological replicates, each with three technical repeats, were conducted for expression pattern analysis.

Quantitative Real-Time PCR (qRT-PCR). The transcription levels of *CarE001A* and *CarE001H* were determined by qRT-PCR using a LightCycler 480 II system (Roche, German) with TB Green Premix Ex Taq II kit (Takara, Japan). Each 20 μL of qRT-PCR reaction consisted of 10 μL of TB Green Premix (2×), 0.8 μL of each primer (10 μM), 2 μL of 20× diluted cDNA template, and RNase-free water. Amplifications were conducted as follows: 95 °C for 5 min, followed by 40 cycles of 95 °C for 15 s and 60 °C for 40 s, and a melting curve analysis was then performed to assess the specificity of each reaction. The amplified products were further sequenced to verify the consistency of the target gene. RNase-free water instead of cDNA templates was used as a negative control. Also, RNA without reverse transcription was set as an additional control to monitor the extent genomic DNA contamination. Using serial 10-fold dilutions of the cDNA template, the amplification efficiency (E) of each gene was validated with the following equation: $E = 10^{-1/\text{slope}} - 1$.[32] The

https://dx.doi.org/10.1021/acs.jafc.9b06690
J. Agric. Food Chem. 2020, 68, 3390−3402

primers used for qRT-PCR analysis are shown in Table S2. Relative expression levels of both CarE genes were calculated using the $2^{-\Delta\Delta CT}$ method,[33] with *EF-1α*, *PRS15*, and *ACTA3α* as reference genes.[34]

Bacterial Expression of Fusion Proteins. The CarE open reading frame encoding the mature enzyme without signal peptide sequence was amplified with specific primer sequences containing restriction endonuclease recognition sites (Table S3). The PCR products were first collected by the Universal DNA Extraction kit (TIANGEN, China) and digested by specific endonucleases, followed by purification using the Omega Gel Extraction kit and ligation into the expression vector pET32a (+) (Novagen, Germany). The sequencing-verified plasmids were finally transformed into the *E. coli* BL21 (DE3) competent cells for protein expression according to the method of Li et al.[29] with slight modification. Briefly, a fresh colony containing the recombinant plasmid was use to inoculate 5 mL of Luria-Bertani (LB) broth medium (100 $\mu g \cdot mL^{-1}$ of ampicillin) with shaking at 37 °C at 220 rpm overnight. Four microliters of cell suspension was then used to inoculate 400 mL of LB broth medium (containing 1% casein hydrolysate, 17 mM KH_2PO_4, 72 mM K_2HPO_4, and 100 $\mu g \cdot mL^{-1}$ ampicillin)[35] with incubation at 37 °C at 220 rpm, and the expression of fusion proteins was subsequently induced at 18 °C at 200 rpm for 48 h with 0.2 mM isopropylthiogalactoside (IPTG) when cell growth reached 0.5−0.6. The vector pET32a (+) without insertion of the target DNA was used as a negative control, and the *E. coli* BL21 (DE3) without transformation of plasmid was used as an additional negative control, these two controls were expressed at the same conditions described as above.

Bacterial cells were harvested by centrifugation at 6,000 rpm at 4 °C for 10 min (CF16RX II, Hitachi Ltd., Japan). Cell pellets were washed twice by 25 mM Tris−HCl (pH 8.0), resuspended in 25 mM Tris−HCl (pH 8.0) at a concentration of 1 mL per 200 mg cell (wet weight), and then lysed by sonication in ice (10 s, 30 passes). Cell lysates were centrifuged at 15,000 rpm at 4 °C for 30 min (CF16RX II, Hitachi Ltd., Japan), and the supernatant containing the soluble fusion proteins was carefully harvested and passed through a 0.22 μm filter to remove the cell debris. Aliquots (100 μL) of the isolated enzyme sample (supernatant of cell lysate) were added into a 0.2 mL tube and stored at −70 °C for the following verification of fusion proteins and the assays of CarE activity.

Identification and Quantification of Expressed CarEs. Native polyacrylamide electrophoresis (native PAGE) was carried out according to the protocol described by Bai et al.[36] Gels were stained for CarE activity measurements using 1 mM α-NA and 3 mM Fast Blue RR salt. The identification of fusion proteins was performed by using a 12% SDS-PAGE and Western blot assays. The concentration of fusion proteins in the enzyme samples was estimated according to the Western blot analysis by using the GelQuantNET software from Biochem-Lab Solutions (University of California, San Francisco). The known purified fusion protein CarE001D from the expression of the *E. coli* system in our previous work,[29] in high purity and with known concentration determined through the Bradford method, was used as an internal reference for the quantification of both expressed CarEs in this work.

CarE Activity of Expressed Enzymes toward α-Naphthyl Acetate. Enzymatic activities of both recombinant CarEs against α-NA were screened at 450 nm by using 96-well microplates on a microplate reader (M200 PRO, Switzerland) by the method of Grant et al.[37] and Bai et al.[36] with slight modifications. In brief, first, to optimize the concentration of the enzyme sample for the enzymatic reaction, the reaction mix consisted of 100 μL of serial twofold dilution of enzyme samples and equal volume of the model substrate α-NA at 200 μM (containing 3 mM Fast Blue RR salt). Second, to accurately determine the kinetic properties of CarE001A and CarE001H, each reaction mix contained 100 μL of the optimal dilution of enzyme samples and 100 μL of substrate solution (containing 3 mM Fast Blue RR salt) at different concentrations (8−200 μM). Reactions were all conducted at 30 °C for 5−10 min. Extracts of the empty vector pET32a (+) without insertion of target gene expressed in the *E. coli* BL21 (DE3) and extracts of the *E. coli* BL21 (DE3) cells without transformation of plasmid representing equivalent preharvest cell densities were used as double negative controls in the assays. Kinetic parameters (V_{max} and K_m) were estimated by measuring the initial rate of metabolite (α-naphthol) formation and fitting the rate data to the Michaelis−Menten equation.

Enzyme Inhibition Studies. The inhibition of esterase activity by three pyrethroid insecticides and three organophosphates was measured according to the method of Bai et al.[36] TPP was used as a positive inhibitor control. Briefly, 1 μL of insecticide stocks was added to 99 μL of enzyme sample to give final concentrations of the substrate ranging from 10^{-4} to 10^{4} μM. The mix was preincubated at 30 °C for 10 min, and the remaining activities were then determined after adding 100 uL of α-NA solution (400 μM). The half inhibitory concentrations (IC_{50}) were determined by the trimmed Spearman-Karber method.[38]

Hydrolase Activity of Expressed Enzymes toward Insecticides. The pyrethroid insecticides, β-cypermethrin, λ-cyhalothrin, and fenvalerate, were initially dissolved in absolute acetone as a stock solution of 20 mM and then diluted with 0.1 M sodium phosphate buffer (PBS) pH 7.5 (0.1 M Na_2HPO_4 and 0.1 M NaH_2PO_4) as a working solution of 200 μM before use. Each 100 μL of this substrate solution was dispensed into separated 1.5 mL microfuge tubes and preincubated at 30 °C for 5 min. Reactions were started by adding 100 μL of appropriately diluted enzyme sample to each microfuge tube and incubated at 30 °C for 0 and 120 min. The reactions were then stopped immediately by the addition of 200 μL of absolute acetonitrile to each microfuge tube, followed by vortexing for 3 min. Negative controls were set up in parallel by using 100 μL of heat-inactivated CarE and 100 μL of the extract of the empty vector pET32a (+) without insertion of target gene expressed in the *E. coli* instead of the active enzyme. The samples were then centrifuged at 12,000 rpm for 8 min, followed by passing through a 0.22 μm filter. HPLC analysis of insecticides remaining was performed on a Agilent HPLC 1260 Series equipped with a Symmetry C18 column (250 × 4.6 mm, 5 μm, Waters) by using solvents acetonitrile and water (80:20, v/v) with a 1.0 $mL \cdot min^{-1}$ flow rate. The column temperature and injection volume were set at 30 °C and 20 μL, respectively. The quantity of substrate remaining was detected at 210 nm. The metabolic activity (specific activity) of each enzyme was expressed as nanomoles of substrate loss per minute per milligram protein.

Homology Modeling and Molecular Docking Analyses. Homology modeling was performed by using Phyre2 (Protein Homology/analogY Recognition Engine V 2.0)[39] to obtain the reliable 3D structures of two CarEs. Taking the amino acid sequence of CarE001A and CarE001H as each query, the crystal structure of *Homo sapiens* butyrylcholinesterase (PDB ID: 4TPK, resolution = 2.7 Å) was selected as the appropriate homology template for two CarEs modeling (about 30% homology).[40] Molecular docking studies were performed to investigate the binding mode between the β-cypermethrin and the CarE proteins using Autodockvina 1.1.2.[41] The 3D structure of β-cypermethrin was drawn by ChemBioDraw Ultra 12.0 and ChemBio3D Ultra 12.0 softwares. The AutoDockTools 1.5.6 package was employed to generate the docking input files.[42] The search grid of the CarE001A and CarE001H were both identified as center_x: 4.401, center_y: 10.0, and center_z: 13.912 with dimensions size_x: 15, size_y: 15, and size_z: 15. The value of exhaustiveness was set to 20. For Vina docking, the default parameters were used if it was not mentioned. The best scoring pose as judged by the Vina docking score was chosen, and then an MD study was performed to revise the docking result.

MD Simulations of the β-Cypermethrin-CarE Complex. The Amber 12 and Amber Tools 13 programs were used to perform MD simulations of the constructed β-cypermethrin-CarE complex.[43] MBPPS was first prepared by ACPYPE.[44] Then, the force field "leaprc.gaff" (generalized amber force field) was used to prepare the ligand, while "leaprc.ff12SB" was used for the receptor. The 3D structure of the β-cypermethrin-CarE complex was immersed in a rectangular box with explicit TIP3P water extending at least 10.0 Å boundary using the "SolvateOct" command with the minimum distance between any solute atoms. Equilibration of the solvated complex was done by carrying out a short minimization (500 steps of

https://dx.doi.org/10.1021/acs.jafc.9b06690
J. Agric. Food Chem. 2020, 68, 3390−3402

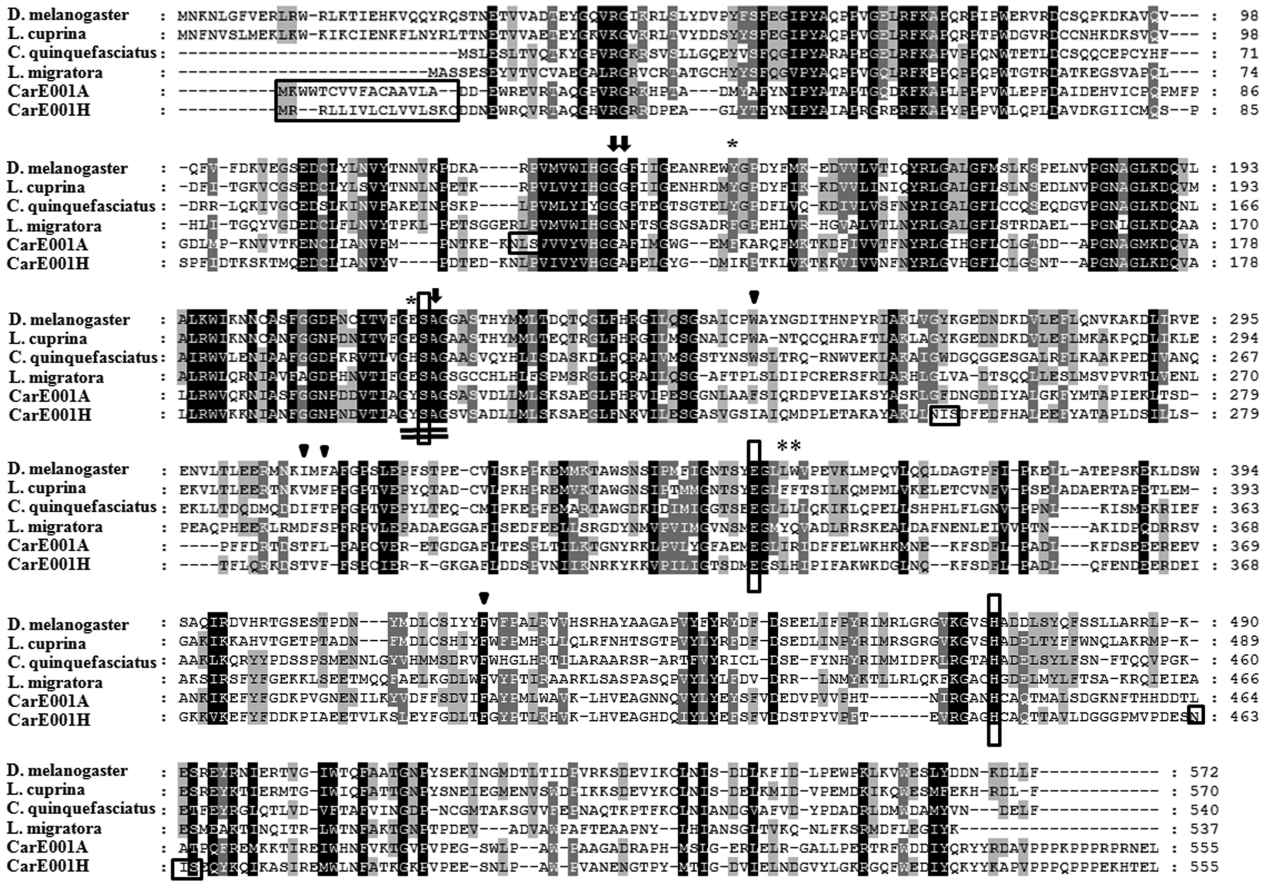

Figure 1. Comparison of the deduced amino acid sequences of CarE001A and CarE001H (GenBank accession numbers: AMO44416.1 and AMO44417.1) from the *H. armigera* WH strain with known insect CarEs: aE7 (GenBank accession number: NP_524261.1) from *D. melanogaster*, E3 (GenBank accession number: AAB67728) from *L. cuprina*, Cqestβ2 and LmCesA5 from *C. quinquefasciatus* (GenBank accession number: CAA83643.1), and *L. migratoria* (GenBank accession number: AGT95756.1), respectively. The signal peptide sequences of CarE001A and CarE001H are presented in the horizontal rectangle, the catalytic triad residues are vertically boxed, the highly conserved pentapeptide residues are marked with double underlines, the oxyanion hole is marked by arrows, the acyl binding pocket is labeled with triangles, the anionic site is shown with asterisks, and the potential N-glycosylation sites are marked with three small horizontal boxes.

each steepest descent and conjugate gradient method), 500 ps of heating, and 50 ps of density equilibration with weak restraints using the GPU (NVIDIA Tesla K20c) accelerated PMEMD module. At last, 20 ns MD simulations were carried out.

■ RESULTS

Cloning and Sequence Analyses of *CarE001A* and *CarE001H*. The complete open reading frames of *CarE001A* and *CarE001H* were obtained and submitted to GenBank (accession numbers: KT345936 and KT345937). Both genes were consisted of 1668 bp, encoding 555 amino acid residues. The predicted molecular weights of protein CarE001A and CarE001H are 62.5 and 62.0 KDa, respectively, and their theoretical isoelectric points are 5.6 and 5.8, respectively. Both CarEs have a signal peptide of 16 amino acids at their N-termini (Figure 1). In addition, CarE001A has one N-glycosylation site of Asn114-Leu115-Ser116, whereas CarE001H has two N-glycosylation sites of Asn254-Ile255-Ser256 and Asn463-Ile464-Ser465. Sequence alignment revealed that both CarE001A and CarE001H had highly conserved catalytic triads (Ser203-His444/443-Glu331/330), pentapeptide motifs (Gly201-X-Ser203-X-Gly205), and other enzymatic active sites in their sequences.

Phylogenetic analyses showed that CarE001A and CarE001H were most phylogenetically related to the *Bombyx* CarEs (Figure S1), which clustered into Clad A all together, an intracellular catalytic class with dietary detoxification functions. Comparison of amino acid sequences of CarE001A and CarE001H with known insect CarEs showed that these two CarEs shared much lower identity (23−28%) with the *Bombyx mori*, *Drosophila melanogaster* aE7, *L. cuprina* E3, *C. quinquefasciatus* estβ2, and *L. migratoria* CesA5. In addition, for BLAST search with the amino acid sequence of each of these two CarEs, the results showed that CarE001A shared about 98% similarity with its alleles from the insecticide susceptible *H. armigera* GR strain and the insecticide resistant YGF strain (Figure S2A) and CarE001H shared 97% identity with its allele from the GR strain (Figure S2B). Notably, CarE001A also shared 97% identity with the acetate esterase HassAE2 (GenBank accession number: ATJ44546) from the pheromone glands of *Helicoverpa assulta*[45] (Figure S2C), suggesting that CarE001A may play multiple roles in *H. armigera*. However, the sequence identity between CarE001A and CarE001H was found to be relatively low (55%) at amino acid levels.

The genomic DNAs of *CarE001A* and *CarE001H* genes (GenBank accession numbers: MN537882 and MN537883) were also obtained through PCR amplifications. Gene sequences of *CarE001A* and *CarE001H* in genome span 2916 and 2170 bp, respectively, and their coding sequences are

https://dx.doi.org/10.1021/acs.jafc.9b06690
J. Agric. Food Chem. 2020, 68, 3390−3402

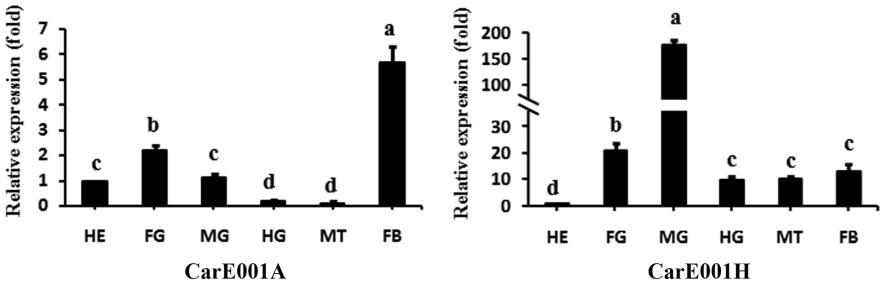

Figure 2. Tissue-dependent expression patterns of *CarE001A* and *CarE001H* in *H. armigera* WH strain. Six different tissues tested: head (HE), foregut (FG), midgut (MG), malpighian tubules (MT), hindgut (HG), and fat body (FB). *EF-1α*, *PRS15*, and *ACTA3α* were used as internal reference genes. Three biological replicates were conducted. Different letters above error bars mean significant differences ($P \leq 0.05$) determined by one-way ANOVA followed by Tukey' s multiple comparison tests.

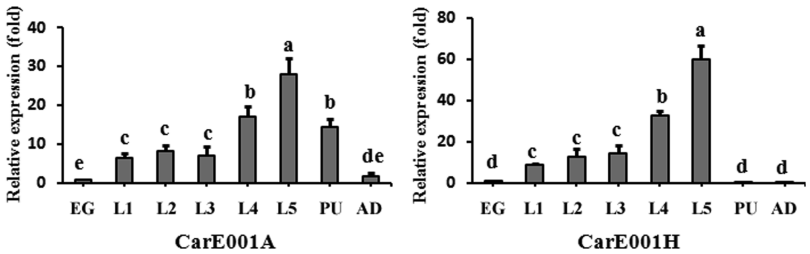

Figure 3. Developmental stage-dependent expression patterns of *CarE001A* and *CarE001H* in *H. armigera* WH strain. Eight different stages were tested: including egg (EG), the first- to fifth-instar larvae (L1−L5), pupae (PU), and adult (AD). *EF-1α*, *PRS15*, and *ACTA3α* were used as reference genes. Three biological replicates were conducted. Different letters above error bars mean significant differences ($P \leq 0.05$) determined by one-way ANOVA followed by Tukey's multiple comparison tests.

comprised of three exons and two introns (Figure S3). The exon/intron size and junctional sequences are detailed in Table S4. No alternative mRNA splicing of *CarE001A* and *CarE001H* was observed in *H. armigera* WH strain.

Tissue-Specific and Developmental Expression Patterns of *CarE001A* and *CarE001H*. The qRT-PCR technique was used to measure transcript levels of *CarE001A* and *CarE001H* in different tissues from the fourth-instar larvae. The transcripts of both CarE genes were detectable in all these body parts examined (Figure 2). In particular, the highest expression of *CarE001A* was found in fat body (6.3-fold), followed by foregut (3.1-fold), midgut (1.1-fold), and head (set as 1.0), and its lowest expression was found in malpighian tubules (0.1-fold). By contrast, *CarE001H* was most abundant in midgut (176.4-fold), followed by foregut (20.9-fold), and fat body (13.2-fold), whereas its lowest expression was found in head (set as 1.0).

The expression patterns of *CarE001A* and *CarE001H* in different life stages were also investigated by qRT-PCR. The results suggested that both CarE genes were widely expressed in all developmental stages of *H. armigera* but with significant variation among different stages (Figure 3). In particular, the expression levels of *CarE001A* and *CarE001H* were relatively higher in the larval stages (between 28- and 59.7-fold) with the highest being found in the fourth- and fifth-instar larvae stages and the lowest in egg and adult stages.

Expression and Identification of Recombinant CarEs. The truncated cDNA sequences encoding *CarE001A* and *CarE001H* without the N-terminal signal peptide were obtained by PCR and ligated into the expression vector pET32a (+) to produce recombinant proteins by using the *E. coli* BL21 (DE3) strain. The Western blot analysis showed the target protein (approximate 75−80 kDa) (Figure 4), which was consistent with the calculated molecular weight (78 KDa)

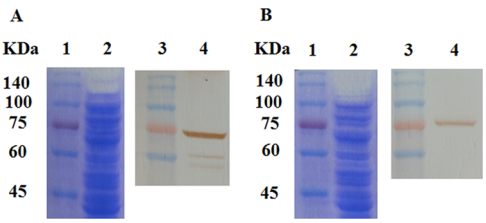

Figure 4. Analysis of recombinant CarEs by SDS-PAGE and Western blot assay. (A) Expression of recombinant CarE001A. (B) Expression of recombinant CarE001H. The samples were separated on 12% gels, and the Western blot analysis was performed with anti-His tag antibody. Lanes 1and 3: protein ladder; Lanes 2 and 4: recombinant proteins of CarE (supernatant of cell lysate) in SDA-PAGE and Western blot assays, respectively.

according to the deduced amino acid sequence of the CarE001A and CarE001H (Trx/6× His/S-tag/CarEs). Following the Western blot assay, native-PAGE was conducted with the generic substrate α-NA to assess whether the recombinant CarEs would have esterase activities. A single clear staining band was detected in the native-PAGE (Figure 5). Taken together, the results suggested that both CarE001A and CarE001H were successfully expressed in the heterologous system, and the recombinant protein could hydrolyze the substrate α-NA into metabolite α-naphthol.

Enzymatic Activity of CarE001A and CarE001H toward α-NA. To measure the catalytic efficiency of CarE001A and CarE001H, kinetic assays were conducted by using a microplate reader (Figures S4 and S5). The kinetic parameters were estimated from the Michaelis−Menten hyperbolic (Figure 6) and are shown in Table 1. Both CarEs had very similar bind affinity toward α-NA with K_m values of 8.6 ± 0.9 and 9.5 ± 1.4 μM. However, CarE001A exhibited

https://dx.doi.org/10.1021/acs.jafc.9b06690
J. Agric. Food Chem. 2020, 68, 3390−3402

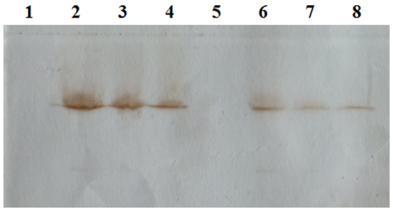

Figure 5. Verification of the CarE activity by native-PAGE staining with α-NA as substrate. Lane 1 and 5: expression of vector PET32a (control); Lane 2–4: 1–3× diluted samples of CarE001A; Lane 6–8: 1–3× diluted samples of CarE001H.

higher catalytic efficiency toward α-NA, with a rate constant (k_{cat}/K_m) of 0.9 ± 0. 1 $s^{-1}\cdot\mu M^{-1}$ and a specific activity of 8.2 ± 0.9 $\mu M\cdot s^{-1}\cdot\mu M^{-1}$ protein. Compared to CarE001A, CarE001H showed a relatively lower enzymatic activity toward α-NA, with a k_{cat}/K_m of 0.6 ± 0.1 $s^{-1}\cdot\mu M^{-1}$ and a specific activity of 4.9 ± 0.5 $\mu M\cdot s^{-1}\cdot\mu M^{-1}$ protein. This is consistent with the stronger staining band of CarE001A versus the weaker staining band of CarE001H observed in the native-PAGE analysis (Figure 5).

Inhibition Analysis. To further characterize the fusion protein of CarE001A and CarE001H, the inhibition of three pyrethroids and three organophosphates on the enzyme activity was determined (Figure 7), and the calculated IC_{50} values are presented in Table 2. Chlorpyrifos, parathion-methyl, and paraoxon-ethyl exhibited much higher inhibition on the activities of both enzymes than the positive control inhibitor TPP, with the IC_{50} values varying from 0.01 to 70 μM. Among these organophosphates, paraoxon-ethyl exhibited strongest inhibition toward CarE001A and CarE001H, with IC_{50} values of 0.016 and 0.019 μM, respectively. However, notably, three types of pyrethroids including β-cypermethrin, λ-cyhalothrin, and fenvalerate showed relative weak inhibition on the activities of both CarEs, with IC_{50} values being higher than 1000 μM. These results suggested that organophosphates are highly binding to CarEs than pyrethroids and also revealed that both CarEs from *H. armigera* were significantly more sensitive to organophosphates.

Metabolic Activity of CarE001A and CarE001H toward Pyrethroid Insecticides. The HPLC assays were performed to assess the ability of CarE001A and CarE001H in metabolizing three pyrethroid insecticides (Figure S6). Their metabolic activities were calculated by monitoring substrate loss and are shown in Figure 8. The results showed that CarE001A could metabolize β-cypermethrin and λ-cyhalothrin, with the specific activities of 3.7 ± 0.7 and 1.0 ± 0.2 nM·$min^{-1}\cdot mg^{-1}$ protein, respectively (Figure 8A). Compared to CarE001A, CarE001H showed relatively lower metabolic activity toward β-cypermethrin and λ-cyhalothrin, with the specific activities of 1.8 ± 0.3 and 0.9 ± 0.2 nM·$min^{-1}\cdot mg^{-1}$ protein, respectively (Figure 8B). However, both CarEs were not able to metabolize fenvalerate, which are shown by nonsignificant differences between treatment and the negative controls.

Docking Analyses and MD Simulations. To better understand the underlying mechanism of CarEs metabolizing pyrethroid insecticides, the 3D structures of both CarEs were constructed (Figure S7), followed by analyses of their molecular docking with β-cypermethrin. The preferential binding mechanism of CarE001A with β-cypermethrin was determined by 20 ns MD simulations based on the docking results (Figure 9). To explore the dynamic stability of the complex and to ensure the rationality of the sampling strategy, the root-mean-square deviation (RMSD) value of the protein backbone based on the starting structure along the simulation time was calculated and plotted (Figure 9A), and it showed that the complex was stabilized during the simulation.

The theoretical binding mode between β-cypermethrin and CarEA is shown in Figure 9. Compound β-cypermethrin adopted a compact conformation to bind in the pocket of the CarE001A (Figure 9B). Substrate molecules located at the hydrophobic pocket, surrounded by the residues Phe85, Ala125, Met128, Trp130, Met133, Ile334, Phe338, and Met449, forming a strong hydrophobic binding (Figure 9C). Detailed analysis of the complex formed by β-cypermethrin and CarE001A (β-cypermetrin-CarE001A complex) showed that the phenyl group at the terminal of β-cypermethrin formed a cation-π interaction with the residue Arg335 of the anionic site and anion-π interactions with the residues Asp337 and Glu331of the catalytic triad. In addition, the phenyl group at the middle of β-cypermethrin formed π–π stacking interaction with the residue His444 of the catalytic triad. In particular, it was also shown that the residue Try202 of the nucleophilic elbow formed a hydrogen bond (bond length: 2.0 Å) with β-cypermethrin, which probably was a more important interaction between β-cypermethrin and CarE001A (Figure 9C). All these interactions helped β-cypermethrin molecules to anchor in the binding site of the CarE001A.

To explain the metabolic activity difference of CarE001A and CarE001H against pyrethroids at the molecular level, β-cypermethrin was further docked into the binding pocket of CarE001H, and then an MD study was performed to revise the docking result (Figure 10). The complex was stabilized during the 20 ns simulation (Figure 10A), and the theoretical binding

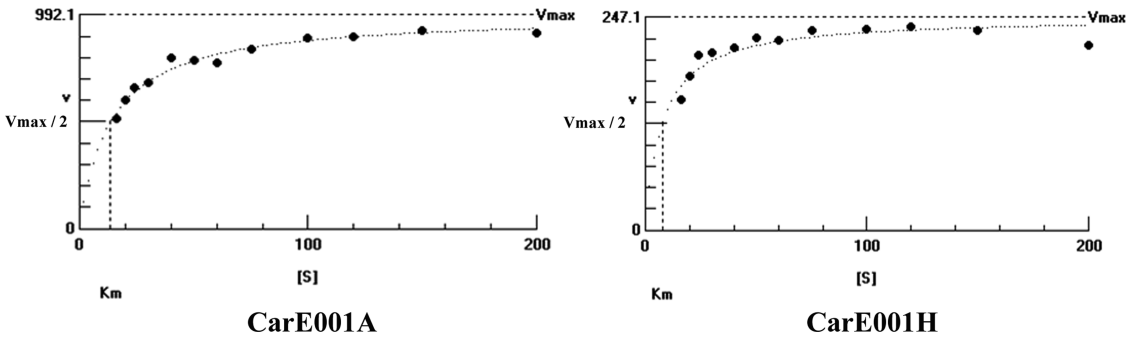

Figure 6. Kinetic enzyme-catalyzed reaction curves. The α-NA was used as a substrate at final concentrations ranging from 16 to 200 μM. V, velocity ($\mu M\cdot s^{-1}$); V_{max}, maximum velocity; [S] , concentration of substrate (μM); K_m, Michaelis–Menten constant (μM).

https://dx.doi.org/10.1021/acs.jafc.9b06690
J. Agric. Food Chem. 2020, 68, 3390–3402

Table 1. Kinetic Parameters of Recombinant CarEs Expressed in *E. coli* toward α-NA[a]

enzyme	V_{max} (nM·s^{-1})	K_m (μM)	k_{cat} (s^{-1})	k_{cat}/K_m (s^{-1}·μM^{-1})	specific activity (μM·s^{-1}·μM^{-1})
CarE001A	1021.3 ± 77.4	9.5 ± 1.4	8.6 ± 0.7	0.9 ± 0. 1	8.2 ± 0.9
CarE001H	254.2 ± 21.6	8.6 ± 1.9	5.1 ± 0.3	0.61 ± 0.1	4.9 ± 0.5
vector	5.3 ± 1.2	-	-	-	-
E. coli	4.1 ± 0.6	-	-	-	-

[a]The expression of vector pET32a without insertion of the target gene and the *E. coli* BL21 (DE3) without transformation of plasmid were used as double negative controls. V_{max}, maximum velocity; K_m, Michaelis−Menten constant; k_{cat}, catalytic constant; k_{cat}/K_m, rate constant; specific activities (at 200 μM substrate). Values are means with standard errors (±SE) based on three replicates. "-" indicates no data available.

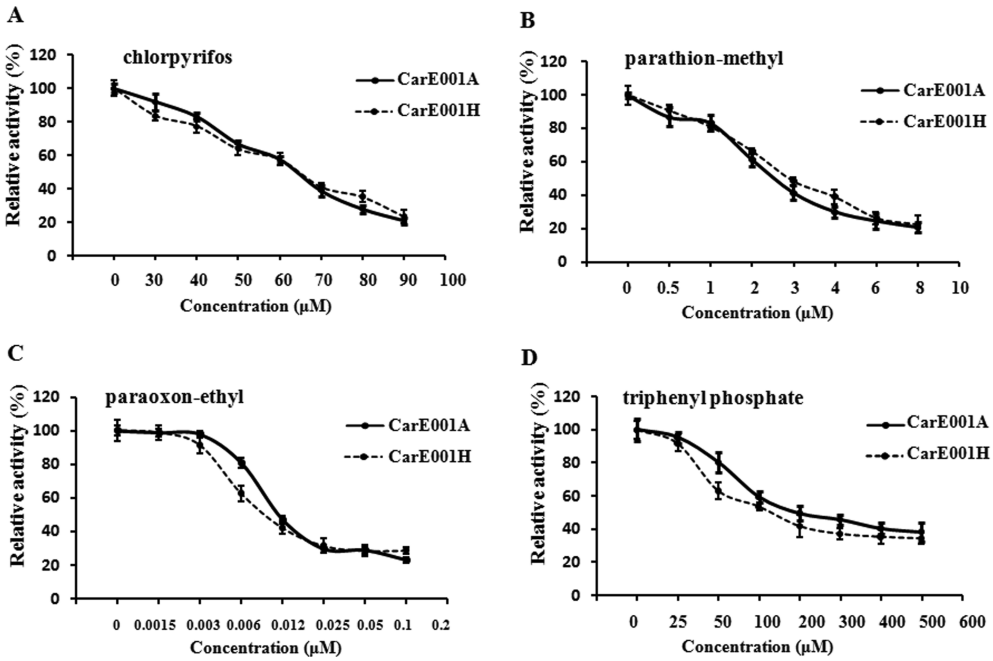

Figure 7. Inhibition tests of insecticides and triphenyl phosphate (TPP) on CarE activities. (A) Chlorpyrifos. (B) Parathion-methyl. (C) Paraoxon-ethyl. (D) TPP. The α-NA was used as a substrate, and TPP was used as a positive control inhibitor. Residual activity was expressed as the percentage of the initial activity without insecticide.

mode between β-cypermethrin and CarE001H is shown in Figure 10B,C. The interaction between β-cypermethrin and CarE001H was very similar to the *CarE001A*. The main difference was that the length of the hydrogen bond (bond length: 2.0 Å) formed between β-cypermethrin and the residue Tyr202 of CarE001A was shorter than that of CarE001H (bond length: 3.0 Å), which probably made *CarE001A* more active toward β-cypermethrin than that of CarE001H. Taken together, the above MD simulations provided a rational explanation of the interaction between β-cypermethrin and both CarEs, which also provided valuable information for further development of CarE inhibitors.

DISCUSSION

Increasing attention has been paid to insect CarEs due to their important roles in the detoxification of endogenous and exogenous compounds including pyrethroids, organophosphates, and carbamates.[10] In this study, two CarE genes were cloned from the *H. armigera* WH strain of China. Sequence comparisons suggest that both CarE001A and CarE001H have highly conserved catalytic triads and pentapeptide motifs, as well as other typical active sites including acyl binding pocket, anionic site, and oxyanion hole (Figure 1). All these indicate that both of them are biological active enzymes. Notably, the similarity of these two CarEs from *H. armigera* with the known CarEs from other insect species appeared very low (23−28%), indicating the substantial divergence of their evolution. CarE001A also shared significantly higher identity (97%) with an acetate esterase HassAE2 exhibiting an antenna-biased expression pattern in *H. assulta*[45] (Figure S2C), suggesting that CarE001A may play multiple roles in *H. armigera*. Additionally, we found that the genes of *CarE001A* and *CarE001H* in genome are 2916 and 2170 bp in length, respectively. Both ORFs of them were 1668 bp in length and encoded a 555 aa protein. However, in *B. dorsalis,* the *BdB1* gene is 10,887 bp in length and contains an ORF of 1953 bp (encoding a 650 aa protein).[46] This indicates that the genomic genes of both *H. armigera* CarEs are significantly smaller in size than *B. dorsalis B1*. Thus, suggesting that insect CarE ORFs are similar in length, whereas the genomic gene sequences of CarEs can be significantly different in size among different insects.

A differential expression pattern of specific CarE genes in different tissues of insects may have implications for their biological functions.[13,47,48] Some studies have demonstrated that CarE genes in most insects are mainly expressed in major detoxifying tissues like the midgut, fat body, and malpighian tubules. In our study, tissue-specific expression patterns of both CarE genes were examined by using qRT-PCR. The highest expression levels of *CarE001A* were observed in fat body, followed by foregut and midgut. However, the tissue

https://dx.doi.org/10.1021/acs.jafc.9b06690
J. Agric. Food Chem. 2020, 68, 3390−3402

Table 2. IC_{50} Values for Test Insecticides

Insecticide	Structure	IC_{50} (μM) [a]	
		001A	001H
β-cypermethrin	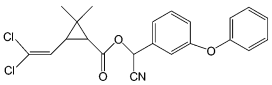	>1000	>1000
λ-cyhalothrin	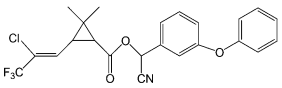	>1000	>1000
Fenvalerate	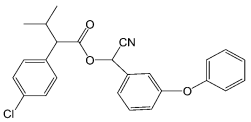	>1000	>1000
Chlorpyrifos	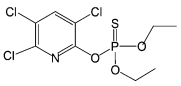	62.0 ± 5.1	64.9 ± 4.7
Parathion-methyl	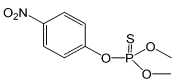	2.4± 0.2	2.9 ± 0.2
Paraoxon-ethyl	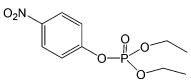	0.016 ± 0.002	0.019 ± 0.005
Triphenyl phosphate[b]	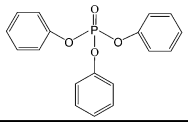	132.9 ± 6.7	154.5 ± 8.9

[a]Concentration of inhibitor that inhibits 50% of the initial enzyme activity; values are means (±SE) based on three replicates. [b]Triphenyl phosphate was used as a positive control inhibitor in this work.

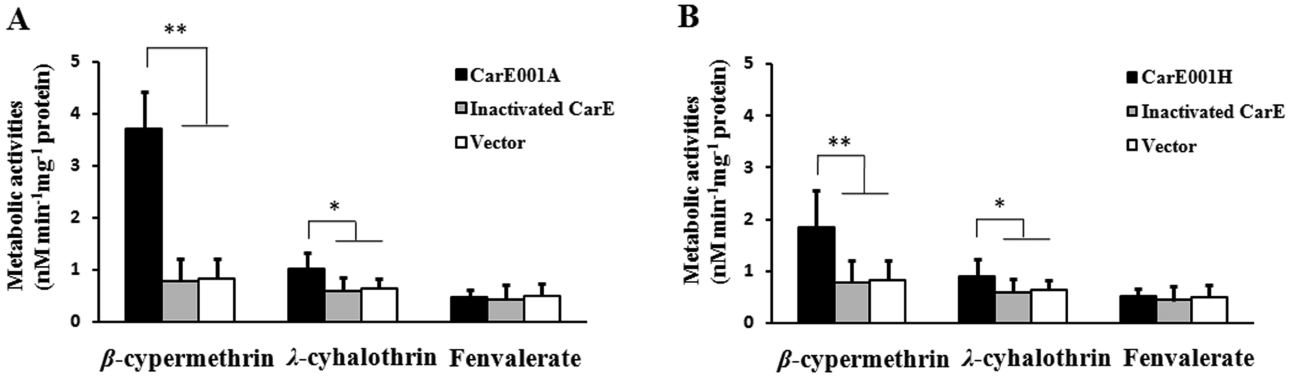

Figure 8. Metabolic activities of CarEs toward three pyrethroids. (A) CarE001A. (B) CarE001H. The values are shown as nanomoles of substrate hydrolyzed by per milligram of enzyme per minute ($nM \cdot min^{-1} \cdot mg^{-1}$ protein). They are means with standard errors based on an average of three replicates. Heat-inactivated proteins of CarE and the sample of vector pET32a expressed in *E. coli* were used as double negative controls. The statistic *t*-test was done for the pair comparison between CarE and controls. Asterisks on the error bars indicate the significant differences identified by student's *t*-test (**$P \leq 0.01$; *$P \leq 0.05$).

expression pattern of *CarE001H* was very different from that of *CarE001A*, because *CarE001H* had the highest expression levels in midgut, followed by foregut and fat body. In the previous study, *LmCesA4* from *L. migratoria*, which has been demonstrated to be associated with three types of insecticide detoxifications, was also found to be highly expressed in fat body.[13] In addition, the CarE gene *BdB1* from the both malathion susceptible and resistant *B. dorsalis* strains had the highest expression level in midgut, followed by head and fat body.[46] It has been well known that insect midgut as the first barrier of toxic compounds from their food plays a key role in metabolism of toxic compounds; fat body is another important tissue with the function of insecticide detoxification, particularly involving insect hormones degradation.[49] Thus, the tissue expression patterns reveal that both CarE genes might imply crucial roles in detoxification of xenobiotic compounds, and *CarE001A* likely also plays a role in insect hormone degradation.

Some studies have demonstrated that the developmental stage-dependent expression profiles of CarEs were highly diverse in different insect species.[13,46] To understand the developmental stage-specific expression profiles of CarE genes

https://dx.doi.org/10.1021/acs.jafc.9b06690
J. Agric. Food Chem. 2020, 68, 3390−3402

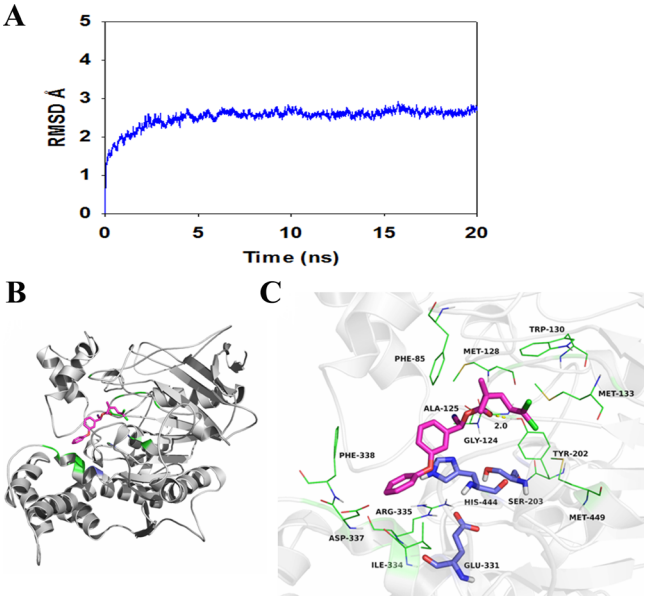

Figure 9. Molecular dynamics (MD) simulations of the β-cypermethrin-CarE001A complex. (A) RMSD values for β-cypermethrin-CarE001A complex during 20 ns MD simulations. (B, C) The predicted binding mode of β-cypermethrin-CarE001A complex was shown by illustration in the surface mode and cartoon mode. The insecticide molecule is presented by rose red sticks. CarE001A was represented with cartoon and the representative binding residues are shown in green lines. The catalytic triad (Ser-Glu-His) are represented with slate sticks. The hydrogen bonds are shown in yellow dotted lines.

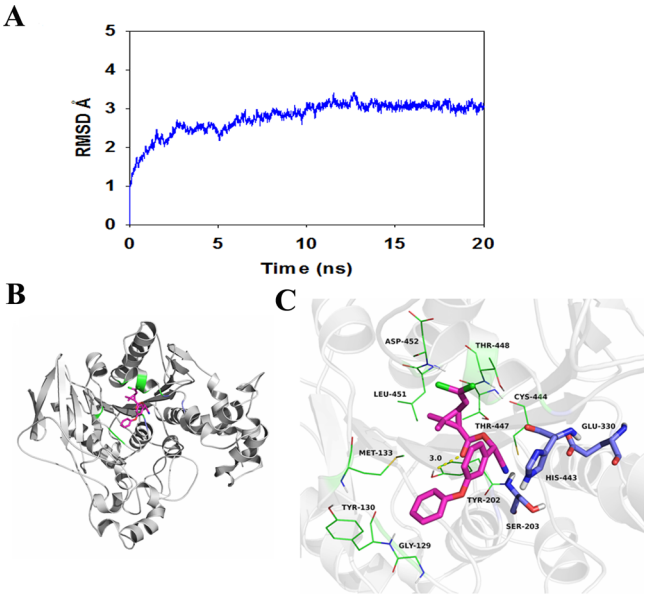

Figure 10. Molecular dynamics (MD) simulations of the β-cypermethrin-CarE001H complex. (A) RMSD values for β-cypermethrin-CarE001H complex during 20 ns MD simulations. (B, C) The predicted binding mode of β-cypermethrin-CarE001H complex was shown by illustrated in the surface mode and cartoon mode. The insecticide molecule is presented by rose red sticks. CarE001H is represented with cartoon, and the representative binding residues are shown in green lines. The catalytic triad (Ser-Glu-His) is represented with slate sticks. The hydrogen bonds are shown in yellow dotted lines.

in *H. armigera*, the expression patterns of both *CarE001A* and *CarE001H* in eight different life stages were also determined by using of qRT-PCR. In the present study, both CarE expression levels in whole body of *H. armigera* were highly expressed in the fourth- and fifth-instar larvae, with the highest level in the fifth-instar larvae than in other life stages, especially egg and adult stages. The expression patterns suggest the potential involvement of both CarEs in detoxification of toxic compounds including insecticides during the main feeding period (fourth- and fifth-instar larvae). By contrast, in *B. dorsalis*, the transcripts of *BdCarE4*, *BdCarE6*, and *BdB1* were all abundant in the adult stage, and relatively low in the egg, larvae, and pupa stages.[20,46] The changing trend of stage-specific expression profiles of both CarEs in *H. armigera* appeared to be dramatically different from *B. dorsalis*. In fact, in *B. dorsalis*, the high expression levels of CarEs in the adult stage are well illustrated that they probably play key roles in the dietary detoxification due to its relatively long life span in the adult stage with a long feeding period. Additionally, in our work, the mRNA of *CarE001A* was also abundant in the pupa stage in *H. armigera*, which might indicate that *CarE001A* plays other unknown roles in metabolism.

The substrate α-NA is commonly used as a model substrate in CarE activity assays. Several studies demonstrated that the BdCarE4, BdCarE6, and BdB1 from *B. dorsalis* showed enzymatic activities with specific activity between 2.5 and 5.2 $nM \cdot min^{-1} \cdot mg^{-1}$ protein toward α-NA, but their kinetic properties still remain unknown.[20,46] In this study, the kinetic analyses of CarE001A and CarE001H were performed through the continuous microplate assay (Figures S4 and S5) according to the protocol of Grant et al.[37] The CarE001A exhibited high catalytic efficiency with a K_m of 9.5 ± 1.3 μM and k_{cat} of 8.6 ± 0.7 s^{-1}, which is rather similar to the kinetic properties of the previously reported *H. armigera* CarE001G with a K_m of 9.6 ± 1.8 μM and k_{cat} of 8.8 ± 0.8 s^{-1}.[36] Compared to CarE001A, CarE001H exhibited relatively lower catalytic efficiency toward α-NA, with a K_m of 8.6 ± 1.9 μM and k_{cat} of 4.9 ± 0.5 s^{-1}. However, both CarE001A and CarE001H showed significantly higher enzymatic activity toward α-NA than another pyrethroid metabolizing CarE from *H. armigera*, which has a K_m of 7.6 ± 0.6 μM and k_{cat} of 2.3 ± 0.1 s^{-1}.[29] Therefore, in this study, the recombinant CarE001A and CarE001H exhibited relatively high hydrolysis activities toward the generic substrate α-NA in the kinetic assay, respectively, indicating that they may have the potential ability to metabolize pyrethroid insecticides since most commonly commercial pyrethroids are carboxyl esters.

To better understand the biochemical properties of the CarEs, inhibition studies were performed following the kinetic assay. The results reveal that β-cypermethrin, λ-cyhalothrin, and fenvalerate exhibited relatively poor inhibition on the enzymatic activity of both CarEs with IC_{50} values over than 1000 μM. However, three organophosphate insecticides including chlorpyrifos, parathion-methyl, and paraoxon-ethyl exhibited more stronger inhibition on the activity of both CarEs (IC_{50}, 0.016 ± 0.002−62.0 ± 5.1 μM) than those of the pyrethroids. The results reveal that both CarE001A and CarE001H were most sensitive to organophosphate insecticides. Similar inhibition properties were also observed in previous studies on CarEs of *H. armigera*,[36] three types of pyrehtroids exhibited relatively lower inhibition on the CarE001G of IC_{50} values of 501.2 ± 22.7 to 612.3 ± 28.4 μM), but other three types of organophosphates displayed

https://dx.doi.org/10.1021/acs.jafc.9b06690
J. Agric. Food Chem. 2020, 68, 3390−3402

most strongest inhibition with IC_{50} values of 0.02 ± 0.00 to 80.7 ± 4.5 μM. CarE is specific in the hydrolysis of carboxylic ester, thus they could hydrolyze agricultural chemicals containing the carboxylic esters. Most commercially used synthetic pyrethroids are carboxyl esters, but most of the commercially registered organophosphates are noncarboxylic esters. Therefore, the organophosphates are usually tight-binding inhibitors to CarEs and potentially lead to aging of most enzymes following phosphorylation.[10] This may explain why *H. armigera* CarEs appeared more sensitive to organophosphates in our previous and present work.

The most important function of CarEs is to metabolize toxic compounds including insecticides. Some studies have provided evidence that insect CarEs were able to metabolize commonly commercial pyrethroids. For example, in an Australian cotton bollworm strain, the crude homogenates from the whole body of larvae exhibited metabolic activity toward esfenvalerate.[27] The preparation of enriched a few CarEs from tissues of a Chinese cotton bollworm strain was found to metabolize fenvalerate by using HPLC analyses.[18] To our best knowledge, to date, our understanding of the capacity of individual CarEs in metabolism of insecticides in *H. armigera* is very limited. In the present study, to investigate whether individual CarE could metabolize pyrethroids, the HPLC assays were further performed with selected commercial pyrethroids, including β-cypermethrin, λ-cyhalothrin, and fenvalerate. Our results demonstrated that both CarE001A and CarE001H were able to metabolize β-cypermethrin and λ-cyhalothrin, and the former showed higher metabolic activity than the latter (Figure 8). Additionally, their metabolic activities against β-cypermethrin and λ-cyhalothrin are also in good accordance with their expression profiles in tissues and developmental stages due to the most abundant of their transcripts in major detoxifying tissues (i.e., fat body and midgut) and main feeding period (i.e., fourth- and fifth-instar larvae). Therefore, our results provide new knowledge for understanding the roles of specific CarEs in metabolizing pyrethroids in *H. armigera*.

We also noted that both CarEs failed to metabolize fenvalerate, whereas in the previous studies, it was shown that fenvalerate could be metabolized by other two *H. armigera* CarEs, CarE001D and CarE001G expressed in the *E. coli*.[29,36] Additionally, CarE001A and CarE001H also appeared clearly different from another previous report of Wu et al.[18] in which two purified esterases preparations (zone A and zone B) have been demonstrated to be able to metabolize fenvalerate with the specific activities of 2.9 and 1.1 $nM \cdot min^{-1} \cdot mg^{-1}$ protein, respectively. One possible reason may be due to the different chemical structures of the three pyrethroids. Another possible reason is that different specific CarEs from the same insect species (i.e., *H. armigera*) probably play different roles in detoxification of various insecticides. The variation of hydrolase activity of different CarEs from the same insect species has been confirmed in another insect species, *L. migratoria*, where it was demonstrated that the esterase LmCesA4 was involved in deltamethrin hydrolysis, but another esterase (LmCesA5) was not.[13] Thus, different individual CarEs play different roles in detoxification of different types of insecticides, which is probably a common phenomenon among various insect species.

Notably, some CarEs from other insect species were found to be associated with detoxification of organophosphates, such as CpCE-1 from *C. pomonella*[14] that could metabolize acephate and BdB1 from *B. dorsalis* (Hendel)[46] that was probably involved in detoxification of malathion. Moreover, other studies have documented that some CarEs could have completely different functions in insects, for example, EST-6 from *D. melanogaster* is a odorant-degrading enzyme toward food odorants[48] and SexiCXE14 from *Spodoptera exigua* displayed activity in degrading either sex pheromones or host plant volatiles.[47] Combining our results, it suggests that CarEs can play various important physiological roles in different insect species.

Our docking analysis and MD simulation results were in accordance with the abovementioned metabolism analyses. As the most important active site of the CarE superfamily (similar with the serine proteases), the highly conserved catalytic triad residues (i.e., Ser-His-Glu) are primarily responsible for catalyzing the hydrolysis of ester groups of the insecticides.[11] It is well known that the first step of CarEs' hydrolyzing their substrates is through the oxygen of the key residue Ser in the catalytic triad making nucleophilic attack on the carbonyl carbon of the substrate.[11] In this work, the 3D structures of CarE001A and CarE001H were generated by using the Phyre2 (Figure S7). Based on this, further insecticide docking analyses and MD simulations demonstrated that β-cypermethrin molecules were anchored in the active site pockets of both CarEs (Figures 9 and 10). The results showed that the β-cypermethrin molecules were surrounded and stabilized through some hydrophobic amino acids in the acyl binding pocket, anionic site, and oxyanion hole. Importantly, the amino acid residual Tyr202 of the highly conserved pentapeptide in both CarEs is predicted to be more close to the carbonyl oxygen atom of ester group of β-cypermethrin with a distance of 2.0−3.0 Å. These analyses can provide a theoretically rational explanation for that CarE001A and CarE001H were capable of hydrolyzing β-cypermethrin. In *L. cuprina*, the LcaE7 model demonstrated that the ability of organophosphates detoxification was largely due to the highly asymmetrical and hydrophobic binding cavity of the esterase aE7.[24] Structure analysis of wild-type E3 showed that three amino acid mutations increased the volume of the acyl binding pocket and led to enhancement of deltamethrin metabolism.[35] However, different from *L. cuprina*, the binding model of *A. gossypii* CarE indicated that amino acid substitutions likely decreased the volume of the catalytic pocket, leading to more amino acids direct and tight interaction with insecticides, thus this could provide a more favorable chemical environment for the substrate.[6] Above differences may also suggest that the optimal volume of active pocket for binding with insecticides is related to different amino acids of the active pocket in a specific enzyme, as well as different chemical compounds like organophosphates and pyrethroids with different molecule sizes and stereostructures. This may also account for the varied metabolic activities of CarEs against different insecticides among insect species. However, to deeply understand the mechanism of interaction between specific CarE and insecticide, the attempts to purify and crystallize CarE, as well as to construct a lot of mutagenesis for both crystal structure and docking analyses, are expected in future study.

Taken together, these results strongly suggest that both CarE genes in *H. armigera* play important roles in the detoxification of pyrethroids, such as β-cypermethrin and λ-cyhalothrin. The further study would focus on understanding the mechanism of detoxification through a combination of creating a large amount of mutations of both CarEs and determining their crystal structures by crystallization.

https://dx.doi.org/10.1021/acs.jafc.9b06690
J. Agric. Food Chem. 2020, 68, 3390−3402

■ ASSOCIATED CONTENT

Supporting Information

The Supporting Information is available free of charge at https://pubs.acs.org/doi/10.1021/acs.jafc.9b06690.

Primers used for cloning of genes, qRT-PCR, and recombinant plasmids (Table S1−S3); the exon/intron size and junctional sequences of genomic CarE genes (Table S4); phylogenetic relationship of insect CarEs (Figure S1); comparison of amino acid differences between the CarE alleles (Figure S2); sequence analysis of genomic gene and mRNA of *CarE001A* and *CarE001H* (Figure S3); enzymatic reaction and kinetic assays of recombinant CarEs with substrate α-NA (Figure S4 and S5); liquid chromatograms at different times in the assay of metabolic activity with three pyrethroids (Figure S6); three dimensional (3D) structures of CarE001A and CarE001H (Figure S7) (PDF)

■ AUTHOR INFORMATION

Corresponding Author

Zhi-Qing Ma − *State Key Laboratory of Crop Stress Biology for Arid Areas, College of Plant Protection, Northwest A&F University, Yangling, Shaanxi 712100, China; Engineering and Research Center of Biological Pesticide of Shaanxi Province, Yangling, Shaanxi 712100, China;* orcid.org/0000-0001-7980-0841; Phone: 86-13709266095; Email: zhiqing-ma@hotmail.com

Authors

Yong-Qiang Li − *State Key Laboratory of Crop Stress Biology for Arid Areas, College of Plant Protection, Northwest A&F University, Yangling, Shaanxi 712100, China;* orcid.org/0000-0001-6023-8238

Li-Sha Bai − *State Key Laboratory of Crop Stress Biology for Arid Areas, College of Plant Protection, Northwest A&F University, Yangling, Shaanxi 712100, China*

Cai-Xia Zhao − *State Key Laboratory of Crop Stress Biology for Arid Areas, College of Plant Protection, Northwest A&F University, Yangling, Shaanxi 712100, China*

Jing-Jing Xu − *State Key Laboratory of Crop Stress Biology for Arid Areas, College of Plant Protection, Northwest A&F University, Yangling, Shaanxi 712100, China*

Zhong-Juan Sun − *State Key Laboratory of Crop Stress Biology for Arid Areas, College of Plant Protection, Northwest A&F University, Yangling, Shaanxi 712100, China*

Yan-Ling Dong − *College of Plant Protection, Northwest A&F University, Yangling, Shaanxi 712100, China*

De-Xian Li − *College of Plant Protection, Northwest A&F University, Yangling, Shaanxi 712100, China*

Xi-Li Liu − *State Key Laboratory of Crop Stress Biology for Arid Areas, College of Plant Protection, Northwest A&F University, Yangling, Shaanxi 712100, China*

Complete contact information is available at: https://pubs.acs.org/10.1021/acs.jafc.9b06690

Funding

This work was supported by the National Natural Science Foundation of China (grants U1903111 and 31201517) and the Fundamental Research Funds of Northwest Agriculture and Forestry University (grants 2452018109, Z1090219003, and 2452015013).

Notes

The authors declare no competing financial interest.

■ ACKNOWLEDGMENTS

We thank professor De-Guang Liu in Northwest A&F University and Dr. Wei Xu at Murdoch University (Australia) for proof reading the earlier version of this manuscript and also thank Professor Yi-Ping Li in Northwest A&F University for her assistance in dissecting the larvae of *H. armigera* and preparing the illustrations.

■ REFERENCES

(1) Tay, W. T.; Soria, M. F.; Walsh, T.; Thomazoni, D.; Silvie, P.; Behere, G. T.; Anderson, C.; Downes, S. A Brave New World for an Old World Pest: *Helicoverpa armigera* (Lepidoptera: Noctuidae) in Brazil. *PLoS One* **2013**, *8*, No. e80134.

(2) Abd El-Latif, A. O.; Subrahmanyam, B. Pyrethroid resistance and esterase activity in three strains of the cotton bollworm, *Helicoverpa armigera* (Hübner). *Pestic. Biochem. Physiol.* **2010**, *96*, 155−159.

(3) Farnsworth, C. A.; Teese, M. G.; Yuan, G.; Li, Y.; Scott, C.; Zhang, X.; Wu, Y.; Russell, R. J.; Oakeshott, J. G. Esterase-based metabolic resistance to insecticides in heliothine and spodopteran pests. *J. Pestic. Sci.* **2010**, *35*, 275−289.

(4) Wang, Z. G.; Jiang, S. S.; Mota-Sanchez, D.; Wang, W.; Li, X. R.; Gao, Y. L.; Lu, X. P.; Yang, X. Q. Cytochrome P450-Mediated λ-Cyhalothrin-Resistance in a Field Strain of *Helicoverpa armigera* from Northeast China. *J. Agric. Food Chem.* **2019**, *67*, 3546−3553.

(5) Qayyum, M. A.; Wakil, W.; Arif, M. J.; Sahi, S. T.; Saeed, N. A.; Russell, D. A. Multiple Resistances Against Formulated Organophosphates, Pyrethroids, and Newer-Chemistry Insecticides in Populations of *Helicoverpa armigera* (Lepidoptera: Noctuidae) from Pakistan. *J. Econ. Entomol.* **2015**, *108*, 286−293.

(6) Gong, Y. H.; Ai, G. M.; Li, M.; Shi, X. Y.; Diao, Q. Y.; Gao, X. W. Functional characterization of carboxylesterase gene mutations involved in *Aphis gossypii* resistance to organophosphate insecticides. *Insect Mol. Biol.* **2017**, *26*, 702−714.

(7) Joussen, N.; Agnolet, S.; Lorenz, S.; Schone, S. E.; Ellinger, R.; Schneider, B.; Heckel, D. G. Resistance of Australian *Helicoverpa armigera* to fenvalerate is due to the chimeric P450 enzyme CYP337B3. *Proc. Natl. Acad. Sci. U. S. A.* **2012**, *109*, 15206−15211.

(8) Tian, K.; Liu, D.; Yuan, Y.; Li, M.; Qiu, X. CYP6B6 is involved in esfenvalerate detoxification in the polyphagous lepidopteran pest, *Helicoverpa armigera*. *Pestic. Biochem. Physiol.* **2017**, *138*, 51−56.

(9) Wang, W.; Hu, C.; Li, X. R.; Wang, X. Q.; Yang, X. Q. CpGSTd3 is a lambda-Cyhalothrin Metabolizing Glutathione S-Transferase from *Cydia pomonella (L.)*. *J. Agric. Food Chem.* **2019**, *67*, 1165−1172.

(10) Wheelock, C. E.; Shan, G.; Ottea, J. Overview of carboxylesterases and their role in the metabolism of insecticides. *J. Pestic. Sci.* **2005**, *30*, 75−83.

(11) Oakeshott, J. G.; Claudianos, C.; Campbell, P. M.; Newcomb, R. D.; Russell, R. J. 5.10 - Biochemical Genetics and Genomics of Insect Esterases. In *Comprehensive Molecular Insect Science*; Gilbert, L. I., Ed. Elsevier: Amsterdam, 2005; pp 309−381.

(12) Ai, G.; Zou, D.; Shi, X.; Li, F.; Liang, P.; Song, D.; Gao, X. HPLC Assay for Characterizing alpha-Cyano-3-phenoxybenzyl Pyrethroids Hydrolytic Metabolism by *Helicoverpa armigera* (Hübner) Based on the Quantitative Analysis of 3-Phenoxybenzoic Acid. *J. Agric. Food. Chem.* **2010**, *58*, 694−701.

(13) Zhang, J.; Ge, P.; Li, D.; Guo, Y.; Zhu, K. Y.; Ma, E.; Zhang, J. Two homologous carboxylesterase genes from *Locusta migratoria* with different tissue expression patterns and roles in insecticide detoxification. *J. Insect Physiol.* **2015**, *77*, 1−8.

(14) Yang, X. Q.; Liu, J. Y.; Li, X. C.; Chen, M. H.; Zhang, Y. L. Key amino acid associated with acephate detoxification by *Cydia pomonella* carboxylesterase based on molecular dynamics with alanine scanning and site-directed mutagenesis. *J. Chem. Inf. Model.* **2014**, *54*, 1356−1370.

(15) Newcomb, R. D.; Campbell, P. M.; Ollis, D. L.; Cheah, E.; Russell, R. J.; Oakeshott, J. G. A single amino acid substitution converts a carboxylesterase to an organophosphorus hydrolase and confers insecticide resistance on a blowfly. *Proc. Natl. Acad. Sci. U. S. A.* **1997**, *94*, 7464−7468.

(16) Hopkins, D. H.; Fraser, N. J.; Mabbitt, P. D.; Carr, P. D.; Oakeshott, J. G.; Jackson, C. J. Structure of an Insecticide Sequestering Carboxylesterase from the Disease Vector *Culex quinquefasciatus*: What Makes an Enzyme a Good Insecticide Sponge? *Biochemistry* **2017**, *56*, 5512−5525.

(17) Han, Y.; Wu, S.; Li, Y.; Liu, J.-W.; Campbell, P. M.; Farnsworth, C.; Scott, C.; Russell, R. J.; Oakeshott, J. G.; Wu, Y. Proteomic and molecular analyses of esterases associated with monocrotophos resistance in *Helicoverpa armigera*. *Pestic. Biochem. Physiol.* **2012**, *104*, 243−251.

(18) Wu, S.; Yang, Y.; Yuan, G.; Campbell, P. M.; Teese, M. G.; Russell, R. J.; Oakeshott, J. G.; Wu, Y. Overexpressed esterases in a fenvalerate resistant strain of the cotton bollworm, *Helicoverpa armigera*. *Insect Biochem. Mol. Biol.* **2011**, *41*, 14−21.

(19) Small, G. J.; Hemingway, J. Molecular characterization of the amplified carboxylesterase gene associated with organophosphorus insecticide resistance in the brown planthopper, *Nilaparvata lugens*. *Insect Mol. Biol.* **2000**, *9*, 647−653.

(20) Wang, L. L.; Huang, Y.; Lu, X. P.; Jiang, X. Z.; Smagghe, G.; Feng, Z. J.; Yuan, G. R.; Wei, D.; Wang, J. J. Overexpression of two α-esterase genes mediates metabolic resistance to malathion in the oriental fruit fly, *Bactrocera dorsalis* (Hendel). *Insect Mol. Biol.* **2015**, *24*, 467−479.

(21) Zhang, L.; Gao, X.; Liang, P. Beta-cypermethrin resistance associated with high carboxylesterase activities in a strain of house fly, *Musca domestica* (Diptera: Muscidae). *Pestic. Biochem. Physiol.* **2007**, *89*, 65−72.

(22) Gong, Y.-J.; Wang, Z.-H.; Shi, B.-C.; Kang, Z.-J.; Zhu, L.; Jin, G.-H.; Wei, S.-J. Correlation between pesticide resistance and enzyme activity in the diamondback moth, *Plutella xylostella*. *J. Insect Sci.* **2013**, *13*, 1.

(23) Oakeshott, J. G.; Farnsworth, C. A.; East, P. D.; Scott, C.; Han, Y.; Wu, Y.; Russell, R. J. How many genetic options for evolving insecticide resistance in heliothine and spodopteran pests? *Pest Manage. Sci.* **2013**, *69*, 889−896.

(24) Jackson, C. J.; Liu, J. W.; Carr, P. D.; Younus, F.; Coppin, C.; Meirelles, T.; Lethier, M.; Pandey, G.; Ollis, D. L.; Russell, R. J.; Weik, M.; Oakeshott, J. G. Structure and function of an insect α-carboxylesterase (αEsterase7) associated with insecticide resistance. *Proc. Natl. Acad. Sci. U. S. A.* **2013**, *110*, 10177−10182.

(25) Cao, C. W.; Zhang, J.; Gao, X. W.; Liang, P.; Guo, H. L. Differential mRNA expression levels and gene sequences of carboxylesterase in both deltamethrin resistant and susceptible strains of the cotton aphid, *aphis gossypii*. *Insect Sci.* **2008**, *15*, 209−216.

(26) Armes, N. J.; Jadhav, D. R.; DeSouza, K. R. A survey of insecticide resistance in *Helicoverpa armigera* in the Indian subcontinent. *Bull. Entomol. Res.* **1996**, *86*, 499−514.

(27) Gunning, R. V.; Moores, G. D.; Devonshire, A. L. Esterases and esfenvalerate resistance in Australian*Helicoverpa armigera*(Hübner) Lepidoptera:Noctuidae. *Pestic Biochem Physiol.* **1996**, *54*, 12−23.

(28) Pearce, S. L.; Clarke, D. F.; East, P. D.; Elfekih, S.; Gordon, K. H. J.; Jermiin, L. S.; McGaughran, A.; Oakeshott, J. G.; Papanikolaou, A.; Perera, O. P.; Rane, R. V.; Richards, S.; Tay, W. T.; Walsh, T. K.; Anderson, A.; Anderson, C. J.; Asgari, S.; Board, P. G.; Bretschneider, A.; Campbell, P. M.; Chertemps, T.; Christeller, J. T.; Coppin, C. W.; Downes, S. J.; Duan, G.; Farnsworth, C. A.; Good, R. T.; Han, L. B.; Han, Y. C.; Hatje, K.; Horne, I.; Huang, Y. P.; Hughes, D. S. T.; Jacquin-Joly, E.; James, W.; Jhangiani, S.; Kollmar, M.; Kuwar, S. S.; Li, S.; Liu, N.-Y.; Maibeche, M. T.; Miller, J. R.; Montagne, N.; Perry, T.; Qu, J.; Song, S. V.; Sutton, G. G.; Vogel, H.; Walenz, B. P.; Xu, W.; Zhang, H.-J.; Zou, Z.; Batterham, P.; Edwards, O. R.; Feyereisen, R.; Gibbs, R. A.; Heckel, D. G.; McGrath, A.; Robin, C.; Scherer, S. E.; Worley, K. C.; Wu, Y. D. Genomic innovations, transcriptional plasticity and gene loss underlying the evolution and divergence of two highly polyphagous and invasive *Helicoverpa* pest species. *BMC Biol.* **2017**, *15*, 63.

(29) Li, Y.; Liu, J.; Lu, M.; Ma, Z.; Cai, C.; Wang, Y.; Zhang, X. Bacterial Expression and Kinetic Analysis of Carboxylesterase 001D from *Helicoverpa armigera*. *Int J Mol Sci* **2016**, *17*, 493.

(30) Yuan, G.; Gao, W.; Yang, Y.; Wu, Y. Molecular cloning, genomic structure, and genetic mapping of two Rdl-orthologous genes of GABA receptors in the diamondback moth, *Plutella xylostella*. *Arch. Insect Biochem. Physiol.* **2010**, *74*, 81−90.

(31) Kumar, S.; Stecher, G.; Tamura, K. MEGA7: Molecular Evolutionary Genetics Analysis Version 7.0 for Bigger Datasets. *Mol. Biol. Evol.* **2016**, *33*, 1870−1874.

(32) Bustin, S. A.; Benes, V.; Garson, J. A.; Hellemans, J.; Huggett, J.; Kubista, M.; Mueller, R.; Nolan, T.; Pfaffl, M. W.; Shipley, G. L.; Vandesompele, J.; Wittwer, C. T. The MIQE guidelines: minimum information for publication of quantitative real-time PCR experiments. *Clin. Chem.* **2009**, *55*, 611−622.

(33) Livak, K. J.; Schmittgen, T. D. Analysis of Relative Gene Expression Data Using Real-Time Quantitative PCR and the 2−ΔΔCT Method. *Methods* **2001**, *25*, 402−408.

(34) Brun-Barale, A.; Héma, O.; Martin, T.; Suraporn, S.; Audant, P.; Sezutsu, H.; Feyereisen, R. Multiple P450 genes overexpressed in deltamethrin-resistant strains of *Helicoverpa armigera*. *Pest Manage. Sci.* **2010**, *66*, 900−909.

(35) Coppin, C. W.; Jackson, C. J.; Sutherland, T.; Hart, P. J.; Devonshire, A. L.; Russell, R. J.; Oakeshott, J. G. Testing the evolvability of an insect carboxylesterase for the detoxification of synthetic pyrethroid insecticides. *Insect Biochem. Mol.Biol.* **2012**, *42*, 343−352.

(36) Bai, L. S.; Zhao, C. X.; Xu, J. J.; Feng, C.; Li, Y. Q.; Dong, Y. L.; Ma, Z. Q. Identification and biochemical characterization of carboxylesterase 001G associated with insecticide detoxification in *Helicoverpa armigera*. *Pestic. Biochem. Physiol.* **2019**, *157*, 69−79.

(37) Grant, D. F.; Bender, D. M.; Hammock, B. D. Quantitative kinetic assays for glutathione S-transferase and general esterase in individual mosquitoes using an EIA reader. *Insect Biochemistry* **1989**, *19*, 741−751.

(38) Hamilton, M. A.; Russo, R. C.; Thurston, R. V. Trimmed Spearman-Karber method for estimating median lethal concentrations in toxicity bioassays. *Environ. Sci. Technol.* **1977**, *11*, 714−719.

(39) Kelley, L. A.; Mezulis, S.; Yates, C. M.; Wass, M. N.; Sternberg, M. J. E. The Phyre2 web portal for protein modeling, prediction and analysis. *Nat. Protoc.* **2015**, *10*, 845−858.

(40) Brus, B.; Košak, U.; Turk, S.; Pišlar, A.; Coquelle, N.; Kos, J.; Stojan, J.; Colletier, J.-P.; Gobec, S. Discovery, biological evaluation, and crystal structure of a novel nanomolar selective butyrylcholinesterase inhibitor. *J. Med. Chem.* **2014**, *57*, 8167−8179.

(41) Trott, O.; Olson, A. J. AutoDock Vina: Improving the Speed and Accuracy of Docking with a New Scoring Function, Efficient Optimization, and Multithreading. *J. Comput. Chem.* **2010**, *31*, 455−461.

(42) Morris, G. M.; Huey, R.; Lindstrom, W.; Sanner, M. F.; Belew, R. K.; Goodsell, D. S.; Olson, A. J. AutoDock4 and AutoDockTools4: Automated docking with selective receptor flexibility. *J. Comput. Chem.* **2009**, *30*, 2785−2791.

(43) Götz, A. W.; Williamson, M. J.; Xu, D.; Poole, D.; Le Grand, S.; Walker, R. C. Routine Microsecond Molecular Dynamics Simulations with AMBER on GPUs. 1. Generalized Born. *J. Chem. Theory Comput.* **2012**, *8*, 1542−1555.

(44) Sousa da Silva, A. W.; Vranken, W. F. ACPYPE - AnteChamber PYthon Parser interfacE. *BMC Research Notes* **2012**, *5*, 367.

(45) Li, R.-T.; Ning, C.; Huang, L.-Q.; Dong, J.-F.; Li, X.; Wang, C.-Z. Expressional divergences of two desaturase genes determine the opposite ratios of two sex pheromone components in *Helicoverpa armigera* and *Helicoverpa assulta*. *Insect. Biochem. Mol. Biol.* **2017**, *90*, 90−100.

(46) Wang, L. L.; Lu, X. P.; Smagghe, G.; Meng, L. W.; Wang, J. J. Functional characterization of BdB1, a well-conserved carboxylesterase among tephritid fruit flies associated with malathion resistance in

Bactrocera dorsalis (Hendel). *Comp. Biochem. Physiol. C: Toxicol. Pharmacol.* **2017**, *200*, 1−8.

(47) He, P.; Zhang, Y. N.; Li, Z. Q.; Yang, K.; Zhu, J. Y.; Liu, S. J.; Dong, S. L. An antennae-enriched carboxylesterase from *Spodoptera exigua* displays degradation activity in both plant volatiles and female sex pheromones. *Insect Mol. Biol.* **2014**, *23*, 475−486.

(48) Chertemps, T.; Younus, F.; Steiner, C.; Durand, N.; Coppin, C. W.; Pandey, G.; Oakeshott, J. G.; Maïbèche, M. An antennal carboxylesterase from *Drosophila melanogaster*, esterase 6, is a candidate odorant-degrading enzyme toward food odorants. *Front. Physiol.* **2015**, *6*, 315.

(49) Ahmad, S.; Duval, D. L.; Weinhold, L. C.; Pardini, R. S. Cabbage looper antioxidant enzymes: Tissue specificity. *Insect Biochem.* **1991**, *21*, 563−572.

https://dx.doi.org/10.1021/acs.jafc.9b06690
J. Agric. Food Chem. 2020, 68, 3390−3402